MATTER: International Journal of Science and Technology
ISSN 2454-5880

Chaisamphao et al., 2019

Volume 5 Issue 3, pp. 15-27

Date of Publication: 15th November 2019

DOI- https://dx.doi.org/10.20319/mijst.2019.53.1527

This paper can be cited as: Chaisamphao, J., Kiatphuengporn, S., Faungnawakij, K., & Donphai, W., (2019). Methane Dry Reforming Over Montmorillonite Surface Modification Supported Nickel Catalyst. MATTER: International Journal of Science and Technology, 5(3), 15-27.

METHANE DRY REFORMING OVER MONTMORILLONITE SURFACE MODIFICATION SUPPORTED NICKEL CATALYST

Juthasiri Chaisamphao
Interdisciplinary Graduate Program in Sustainable Energy and Resources Engineering, Kasetsart University, Bangkok, Thailand
juthasiri.cha@gmail.com

Sirapassorn Kiatphuengporn
National Nanotechnology Center (NANOTEC), National Science and Technology Development Agency (NSTDA), Pathum Thani, Thailand
sirapassorn.kia@nanotec.or.th

Kajornsak Faungnawakij
National Nanotechnology Center (NANOTEC), National Science and Technology Development Agency (NSTDA), Pathum Thani, Thailand
kajornsak@nanotec.or.th

Waleeporn Donphai
Department of Chemical Engineering, Faculty of Engineering, Kasetsart University, Bangkok, Thailand
Research Network of NANOTEC – KU on NanoCatalysts and NanoMaterials for Sustainable Energy and Environment
fengwod@ku.ac.th

Abstract

Dry reforming of methane has been taken an interest in research and development for converting greenhouse gases (CH_4 and CO_2) into hydrogen (H_2) and carbon monoxide (CO). Clay has been considered as promising materials because of their structure, low cost and wide availability. Different surface modifications of clay directly affect the performance of catalyst in term of CH_4

and CO_2 conversion. This research studied nickel loaded on montmorillonite (MMT) clay support with different surface modifications on the activity in dry reforming of methane in fixed-bed reactor with reactant gases flow rate of 60 ml/min (CH_4:CO_2 of 1) at reaction temperature ranges of 500 – 800°C. Montmorillonite clay support with different surface modifications including trimethyl stearyl ammonium (MMT-TSA), dimethyl dialkyl amine (MMT-DDA), methyl dihydroxy-ethyl hydrogenated tallow ammonium (MMT-MDA) and aminopropyltriethoxysilan and octadecylamine (MMT-AO) were investigated. As the results, the performances of all catalysts increased with increasing reaction temperature because this reaction is endothermic reaction. Among them, Ni/MMT-TSA catalyst exhibited the highest CH_4 and CO_2 conversions at all reaction temperatures due to its high surface area, and high metallic surface area.

Keywords

Dry Reforming of Methane, Nickel, Montmorillonite, Surface Modification, Hydrogen Production

1. Introduction

To deal with increasing energy demand, running out of energy sources, fluctuation of fuel price and climate change, the development of alternative sources of energy is necessary (Talaat Shawky, 2017). Dry reforming of methane is an interesting reaction for converting two major greenhouse gases including methane (CH_4) and carbon dioxide (CO_2) to produce syngas (H_2 and CO). The syngas are used as reactant gases for the production of high-value hydrocarbons and alcohols via Fischer–Tropsch synthesis (Donphai, Faungnawakij, Chareonpanich & Limtrakul, 2014; Faria, Neto, Colman & Noronha, 2014, Zhang et al., 2018; Al-Fatesh et al., 2019). The dry reforming of methane equation is exhibited in Eq. (1).

$$CH_4\,(g) + CO_2\,(g) \rightarrow 2H_2\,(g) + 2CO\,(g) \qquad \Delta H^o = 247\ kJ/mol \qquad (1)$$

Moreover, it was found that the coke deposition on catalyst surface can occurred during this reaction leading to catalytic deactivation. The coke can originate from the methane decomposed to carbon and hydrogen (Eq. (2)) or the carbon monoxide decomposed to carbon and carbon monoxide (Boudouard reaction) (Eq. (3))

$$CH_4\,(g) \rightarrow C\,(s) + 2H_2\,(g) \qquad \Delta H^o = 75\ kJ/mol \qquad (2)$$

$$2CO\,(g) \rightarrow C\,(s) + CO_2\,(g) \qquad \Delta H^o = -171\ kJ/mol \qquad (3)$$

Furthermore, the reverse water gas shift reaction is one important side reaction that consumes H_2 to products (Eq. (4)).

$$CO_2(g) + H_2(g) \rightarrow CO(g) + H_2O(g) \qquad \Delta H^o = -41 \text{ kJ/mol} \qquad (4)$$

The dry reforming of methane is endothermic reaction; therefore, it requires high reaction temperature to perform higher the conversions and syngas yields. In order to reduce the temperature, the appropriate catalyst must be used. The noble metal-based catalysts (Pt, Pd, Rh, Ru) have superior activity and high stability in dry reforming reaction; however, the price of this noble metals are quite high. Therefore, the Ni-based catalyst (non-noble metal catalyst) has been widely used in dry reforming of methane due to its high catalyst performance, low cost and availability (Khajeh Talkhoncheh & Haghighi, 2015; Li, Tian, Zeng, Zhao & Gong, 2016, Shin et al., 2018). However, the Ni-based catalyst is deactivated by coke formation and sintering at high temperatures (Dou et al., 2019). In order to solve these problems, the use of suitable catalyst support with excellent confining structure can be a strategy have been employed to promote the catalytic stability of Ni catalyst (Lu et al., 2018). Montmorillonite (MMT) is an abundant mineral clay that have been considered as a promising materials for being support for dispersing Ni particles. It was due to its laminar structure and sheet-like morphology which desirable dispersion effect and large specific surface areas that it possess (Li, Tang, Song, Jiang & Zhang, 2018; Li, Song, Jiang, Wang & Zhang, 2017; Li, Zhang, Xie, Yin & An, 2015). Therefore, this research studied the effect of nickel loaded on montmorillonite support with different surface modification including, trimethyl stearyl ammonium (MMT-TSA), dimethyl dialkyl amine (MMT-DDA), methyl dihydroxy-ethyl hydrogenated tallow ammonium (MMT-MDA) and aminopropyltriethoxysilan and octadecylamine (MMT-AO), on the activity in dry reforming of methane. The physical and chemical properties of catalyst were characterized by using X-ray powder diffraction (XRD), Fourier-transform infrared spectroscopy (FTIR), N_2 adsorption-desorption, H_2 temperature-programmed reduction (H_2-TPR) and CO chemisorption.

2. Experimental

2.1 Catalyst Preparation

The four types of modified surface montmorillonites including trimethyl stearyl ammonium (MMT-TSA), dimethyl dialkyl amine (MMT-DDA), methyl dihydroxy-ethyl hydrogenated tallow ammonium (MMT-MDA) and aminopropyltriethoxysilan and octadecylamine (MMT-AO) were obtained from Sigma Aldrish in collaboration with Nanocor® and they were used as support of the catalysts.

Ni/MMT-x catalysts were prepared via wet impregnation method. Nickel nitrate hexahydrate ($Ni(NO_3)_2 \cdot 6H_2O$) was dissolved in deionized water. After that, MMT-x powder were added into the nickel nitrate solution, and stirred on hot plate at 60°C for 3 h. The impregnated MMT were then dried at 100°C overnight. Subsequently, the solids were calcined at 500ºC for 3 hours to remove the remaining organic materials and generate NiO.

2.2 Characterization

XRD analysis was employed for crystal phase identification. XRD patterns were recorded on a Bruker D8 Advances X-ray diffractometer using Cu-Kα radiation with a voltage of 40 kV and a current of 40 mA. The textural properties of Ni/MMT-x was investigated by N_2 adsorption desorption isotherm in the NOVA e-Series of surface area analyzer using liquid nitrogen as adsorbent at 77K. Before analysis, the sample were vacuumed degassed at 240ºC for 12 hours.

The crystallite sizes of NiO were calculated by using Scherrer equation (Eq. 5)

$$D = k \frac{\lambda}{\beta cos\theta} \quad (5)$$

Where k = 0.94, λ is the wavelength of the Cu-Kα radiations (λ = 0.15406 nm), β is is the full width at half maximum and θ is the angle obtained from 2θ values corresponding to maximum intensity peak in XRD pattern.

The specific surface area, pore volume and pore diameter were calculated according to Brunauer-Emmett-Teller (BET) and Barrett-Joyner-Halenda (BJH) methods.

FT-IR study was obtained by using Nicolet 6700 spectrometer and collected the sample in the spectra range of 4000-400 cm^{-1}. The sample was prepared as a KBr pellet. MMT powder was previously mixed with KBr around 1:100 ratio and then ground. After that, the sample was pressed by using a hydraulic press.

H_2 temperature-programmed reduction (H_2-TPR) was performed to investigate the reducibility of the catalysts and interaction between metal and the supports by using a temperature programmed heating furnace with gas chromatography to detect H_2 effluent gas. In an experiment, 0.1 g of catalyst was packed in fixed-bed reactor of 3/8" diameter and heated from room temperature to 980ºC with a heating ramp of 5ºC/min. The catalyst was reduced with 9.5%H_2/Ar at 30 ml/min during the TPR test.

CO chemisorption was conducted to determine Ni metallic surface area on Ni/MMT-x catalysts. A sample of 0.2 g was loaded into fixed-bed reactor. Prior to chemisorption, the catalyst was reduced under flow rate of 60 ml/min of H_2 at heating rate of 10ºC/min to 700ºC for 3 hours.

Then, it was flushed with pure Ar gas at 700ºC for 30 min. After that the temperature was reduced to 50ºC and 50 µL of CO pulses were introduced to catalyst until the adsorption peak stable.

The active nickel area were calculated by using the following equation (Eq. 6)

$$A_m = \frac{V_{chem} \cdot 6.02 \times 10^{23} \cdot SF \cdot \sigma_m \cdot 10^{-18} \cdot 100}{c} \quad (6)$$

Where A_m is metal surface area (m^2/g_{Ni}), V_{chem} is chemisorption volume (µmol/g), SF is stoichiometry factor (Ni : CO =1), σ_m is supported metal cross section area and c is supported metal weight %.

2.2 Catalytic activity test

Before the test, 0.1 g of Ni/MMT was loaded in a fixed-bed reactor and reduced at 700ºC in H_2 with a flow rate of 60 ml/min for 3 hours. The reactance gas was kept constant at 50 ml/min with a molar ratio of CH_4: CO_2 of 1:1. The activity test was operated from 500 to 800ºC in step of 50ºC. The effluent gases was analyzed by gas chromatography with a thermal conductivity detector (TCD). The conversion of CH_4 and CO_2 are defined as follows:

$$CH_4 \text{ conversion } (\%) = \frac{[CH_4]_{in} - [CH_4]_{out}}{[CH_4]_{in}} \times 100\% \quad (7)$$

$$CO_2 \text{ conversion } (\%) = \frac{[CO_2]_{in} - [CO_2]_{out}}{[CO_2]_{in}} \times 100\% \quad (8)$$

$$H_2/CO \text{ ratio} = \frac{\text{Mole of } H_2}{\text{Mole of CO}} \quad (9)$$

Where $[CH_4]_{in}$ and $[CO_2]_{in}$ refer to the flow rates of inlet of CH_4 and CO_2, while $[CH_4]_{out}$ and $[CO_2]_{out}$ refer to the flow rate of outlet of CH_4 and CO_2.

The catalyst performance are expressed in terms of the average CH_4 and CO_2 conversions and the H_2/CO ratio during 1 hour of each reaction temperature.

3. Results and Discussion

3.1 Catalyst Characteristics

The XRD patterns of Ni/MMT-x catalysts examined by X-ray diffraction were shown in Figure 1. All catalysts exhibited the same diffraction peaks at 7.0º, 18.2º, 28.5º, 35.0º and 61.7º corresponded to the main mineral component of montmorillonite (Li, Song, Jiang, Wang & Zhang, 2017). While the peaks at 37.3º, 43.4º, 63.0º, 75.6º and 79.6º were represented to the cubic phase of NiO (Abdollahifar, Haghighi & Babaluo, 2014; Ashik & Wan Daud, 2015). The NiO crystallite size of catalysts were calculated according to Scherrer equation and showed in Table 1. It was found that the smallest and largest of NiO crystallite size were observed in the case of Ni/MMT-TSA and Ni/MMT-AO catalysts, respectively.

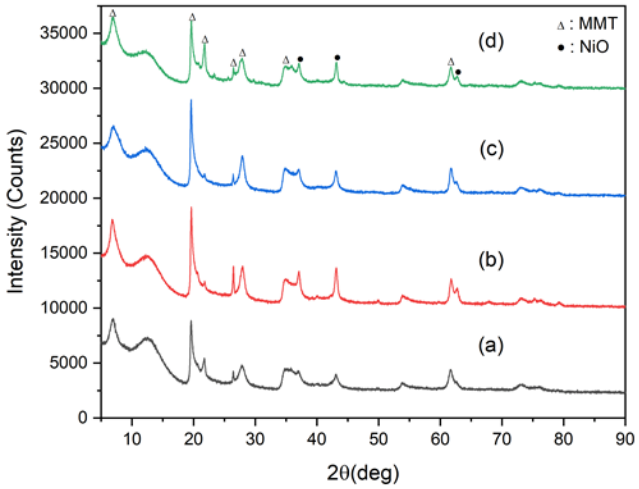

Figure 1: *XRD Patterns of Catalysts*

(a) Ni/MMT-TSA, (b) Ni/MMT-DDA, (c) Ni/MMT-MDA and (d) Ni/MMT-AO

Table 1: *Surface Areas, Pore Diameter, Pore Volume, NiO Crystalline Size and Ni Metallic Surface Area of the Catalysts*

Sample	Surface area [a] (m^2/g)	Smaller pore diameter [a] (nm)	Larger pore diameter [a] (nm)	Pore volume [a] (cm^3/g)	NiO crystallite size [b] (nm)	Active nickel area [c] (m^2/g_{Ni})
Ni/MMT-TSA	91	4.00	20.07	0.24	13.7	1.57
Ni/MMT-DDA	39	3.72	27.40	0.39	19.31	1.62
Ni/MMT-MDA	73	4.01	10.13	0.21	18.39	2.29
Ni/MMT-AO	69	3.98	17.29	0.22	25	0.77

[a] Calculated by using Brunauer-Emmett-Teller (BET) and Barrett-Joyner-Halenda (BJH) methods.

[b] Calculated from Scherrer equation.

[c] Calculated from CO chemisorption data.

The FT-IR spectra of MMT supports are presented in Figure 2. The absorption band observed around 3,630 cm^{-1} indicated the vibration of O-H bond. Asymmetric stretching, symmetric stretching and in-plane scissoring vibrations of methylene group (CH_2) were observed at the two sharp peaks at 2,920, 2,850 and single peak at 1,470 cm^{-1}, respectively. These were the characteristics of montmorillonite surface modified by the alkyl chains of the modifiers (Pugazhenthi, Suresh, Vinoth Kumar, Kumar & Rajkumar Surin, 2018). The adsorption spectrum at 1636 cm^{-1} indicated the hydration and the hydroxyl group bending vibration of water molecules present in the clays. A broader peak at 1,032 cm^{-1} was represented as stretching vibration of Si-O. The peak appeared at 660, 521 and 470 cm^{-1} were designated as Mg-O bond, Al-O stretching and

Si-O bending vibration, respectively (Hayati-Ashtiani, 2011). All the four spectra demonstrated to the different functional groups on the different modified surfaces of MMT-x supports. Higher intensity of peak around 3,400 cm^{-1} of the MMT- DDA support was clearly observed, indicating the H-O-H stretching of structural hydroxyl group and water. The spectra of MMT-AO support showed two small peaks at 3253 and 3187 cm^{-1}, indicating the presence of a primary amine. For MMT-DDA support, there were more amount of alkyl groups on the clay support (Santhini, Sugunalakshmi, Suriyaraj & Bava Bakrudeen, 2018).

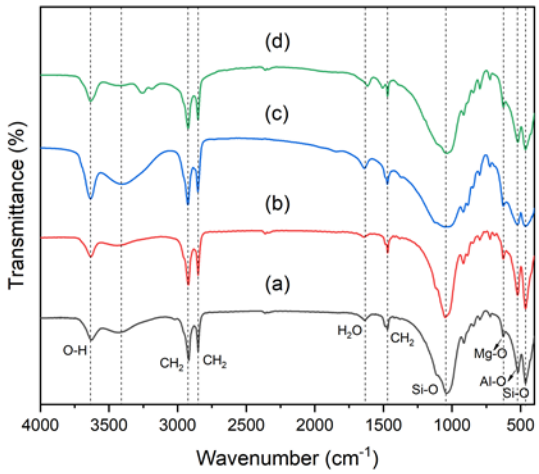

Figure 2: *FT-IR spectra of (a) MMT-TSA, (b) MMT-DDA, (c) MMT-MDA and (d) MMT-AO*

The N_2 adsorption-desorption isotherms of Ni/MMT-x catalysts are presented in Figure 3. All Ni/MMT-x catalysts displayed type IV of isotherm with H3 shaped hysteresis loops, indicating the characteristic of mesoporous structure and aggregation of plate-like particles with slit shaped porous structure according to IUPAC classification. The pore size distribution of these catalysts determined by using BJH desorption are illustrated in Figure 4. It was found that a bimodal pore size distribution was observed for all catalysts. The average smaller and larger pore size of catalysts were located in ranges of 3.72 – 4.01 nm and 10.13 - 27.40 nm, respectively.

The surface area, pore volume and Ni metallic surface area of Ni/MMT-x catalysts are summarized in Table 1. The Ni/MMT-TSA and Ni/MMT-DDA catalysts exhibited the highest and lowest surface area, respectively, among all of catalysts after loaded nickel. It was due to the fact that some NiO particles blocked the pore size of modified montmorillonite clay support. The active nickel area calculated from the results from CO chemisorption are presented in Table 1. The results showed that the active nickel area of all catalysts can be arrange in the order, Ni/MMT-MDA > Ni/MMT-TSA > Ni/MMT-DDA > Ni/MMT-AO.

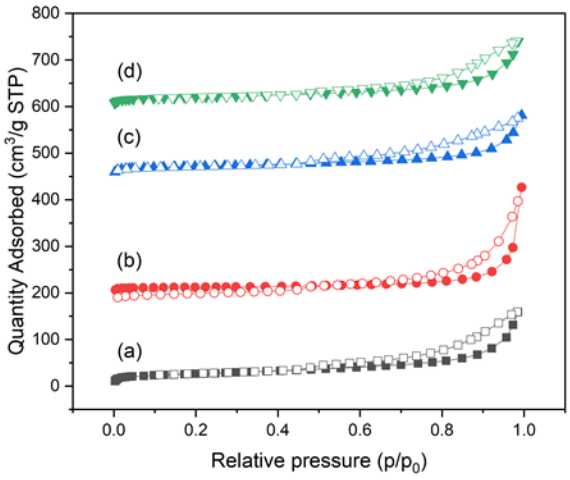

Figure 3: *N_2 Adsorption-Desorption Isotherms of Catalysts*
(a) Ni/MMT-TSA, (b) Ni/MMT-DDA, (c) Ni/MMT-MDA and (d) Ni/MMT-AO

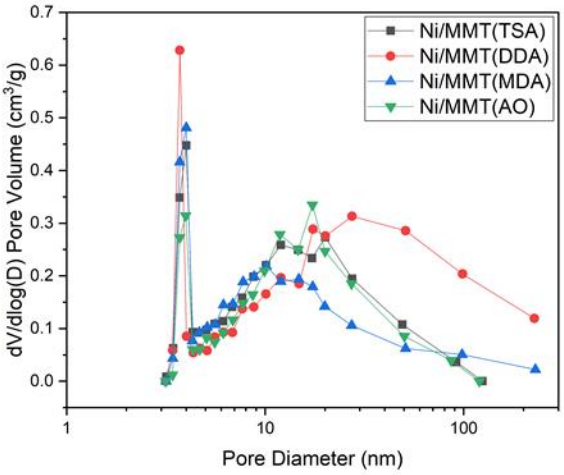

Figure 4: *Pore Size Distribution of Catalysts*
(a) Ni/MMT-TSA, (b) Ni/MMT-DDA, (c) Ni/MMT-MDA and (d) Ni/MMT-AO

H_2-TPR profile of Ni/MMT-x catalysts is shown in Figure 5. Three reduction peaks at different temperature ranges were observed. The first peak around 380ºC was ascribed to the reduction of bulk NiO species on the external surface having a weak interaction with the MMT-x support. While the second peak was attributed to the reduction of encapsulated Ni species in MMT layer that have strong interaction. The last peak at higher temperature around 670 ºC was correspond to the effect of surface modified MMT-x supports and the reducible Ni species in nickel phyllosilicate form or located in the mesoporous structure of the support (YIN, XIE, WU & AN, 2016; Wang et al., 2016). It was found that the reduction peak of Ni/MMT-TSA catalysts shifted to lower temperature at the first peak, indicating the reduction temperature of bulk NiO was weaker

interaction with external surface than other Ni/MMT-x catalysts. The last reduction peak of Ni/MMT-AO catalyst was performed at 737°C, which was much higher than other catalysts, implied the larger size of NiO species required higher temperature and took long time to reduce to active phase and due to stronger interaction between nickel phyllosilicate and the support (Shah, Das, Nayak, Mondal & Bordoloi, 2018). As the results, it could be explained that the different surface modifications of montmorillonite support could affect the characteristics of nickel metal loaded on support in terms of nickel size and the interaction between nickel and support.

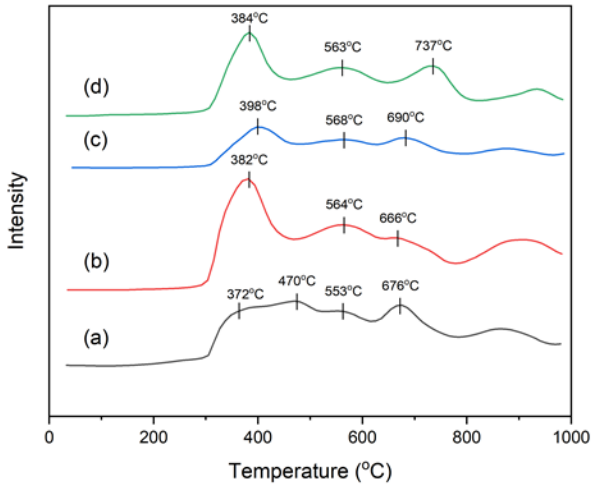

Figure 5: *H_2-TPR Profiles of Catalysts*

(a) Ni/MMT-TSA, (b) Ni/MMT-DDA, (c) Ni/MMT-MDA and (d) Ni/MMT-AO

3.2 Catalytic Performance

The catalytic performance in term of CH_4 and CO_2 conversions of Ni/MMT-x catalysts are illustrated in Figure 6(a) and Figure 6(b), respectively. As the results, the CH_4 and CO_2 conversions increased with the increasing reaction temperature for all catalysts. Moreover, the CO_2 conversion was higher than those of CH_4 conversion because the reverse water gas shift reaction was occurred in the system. The H_2/CO ratio are presented in Figure 6(c). It was found that the H_2/CO ratio for all catalysts is less than 1, which lower than the stoichiometric value for dry reforming of methane reaction because of the influence of reverse water gas shift reaction. Among Ni/MMT-x catalysts, Ni/MMT-TSA catalyst exhibited the highest CH_4 and CO_2 conversions at all reaction temperatures, which could be the effect of highest surface area. In addition, the CH_4 and CO_2 conversions of Ni/MMT-MDA close to the conversions of Ni/MMT-TSA due to the highest metallic surface area.

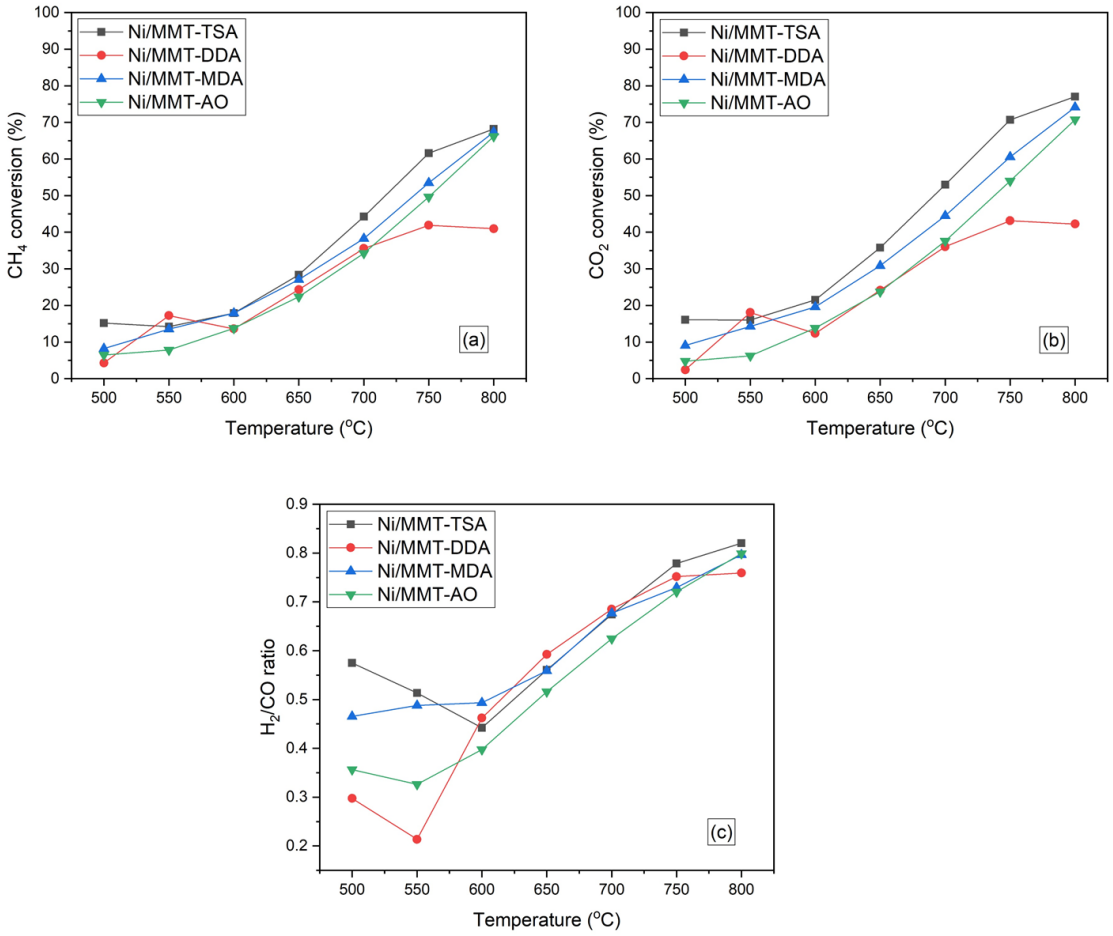

Figure 6: *CH_4 Conversion (a), CO_2 Conversion (b) and H_2/CO Ratio (c) on Ni/MMT Catalysts in Dry Reforming of Methane*

4. Conclusion

In summary, the Ni supported on montmorillonite with different surface modification (MMT-TSA, MMT-DDA, MMT-MDA and MMT-AO) were successfully prepared via wet impregnation method, and test their activities in dry reforming of methane at temperature range of 500 – 800 °C. As the results, the Ni/MMT-TSA catalyst exhibited the highest surface area, followed by Ni/MMT-MDA, Ni/MMT-AO, and Ni/MMT-DDA catalyst, respectively. The highest active nickel area was observed in the case of Ni/MMT-MDA catalyst. It could be explained that the modified surface of montmorillonite directly affected the characteristic of surface and dispersion of nickel particle on catalyst surface. Ni/MMT-TSA catalyst showed the highest CH_4 and CO_2 conversions at all reaction temperatures compared to the other catalysts, due to the effect of high surface area and active nickel area. For the future work, these catalysts will be further

investigated in term of stability by dry reforming of methane reaction at the specified temperature at 750°C for a time on stream of 10 hours.

5. Acknowledgement

The authors gratefully acknowledge the financial supports of Thailand Advanced Institute of Science and Technology (TAIST), National Science and Technology, Kasetsart University under TAIST Tokyo Tech program, National Nanotechnology Center (NANOTEC), National Science and Technology Development Agency (NSTDA), and Department of Chemical Engineering, Faculty of Engineering, Kasetsart University.

References

Abdollahifar, M., Haghighi, M., & Babaluo, A. (2014). Syngas production via dry reforming of methane over Ni/Al_2O_3–MgO nanocatalyst synthesized using ultrasound energy. Journal of Industrial and Engineering Chemistry, 20 (4), 1845-1851. https://doi.org/10.1016/j.jiec.2013.08.041

Al-Fatesh, A., Kumar, R., Kasim, S., Ibrahim, A., Fakeeha, A., & Abasaeed, A. et al. (2019). The effect of modifier identity on the performance of Ni-based catalyst supported on γ-Al_2O_3 in dry reforming of methane. Catalysis Today. https://doi.org/10.1016/j.cattod.2019.09.003

Ashik, U., Daud, W. W. (2015). Stability enhancement of nano-nio catalyst with SiO_2 support to get improved hydrogen yield from methane decomposition. Matter: International Journal of Science and Technology, 2 (1), 42-52. https://doi.org/10.20319/mijst.2016.21.4252

Donphai, W., Faungnawakij, K., Chareonpanich, M., & Limtrakul, J. (2014). Effect of Ni-CNTs/mesocellular silica composite catalysts on carbon dioxide reforming of methane. Applied Catalysis A: General, 475, 16-26. https://doi.org/10.1016/j.apcata.2014.01.014

Dou, J., Zhang, R., Hao, X., Bao, Z., Wu, T., Wang, B., & Yu, F. (2019). Sandwiched SiO_2@Ni@ZrO_2 as a coke resistant nanocatalyst for dry reforming of methane. Applied Catalysis B: Environmental, 254, 612-623. https://doi.org/10.1016/j.apcatb.2019.05.021

Faria, E., Neto, R., Colman, R., & Noronha, F. (2014). Hydrogen production through CO_2 reforming of methane over Ni/$CeZrO_2$/Al_2O_3 catalysts. Catalysis Today, 228, 138-144. https://doi.org/10.1016/j.cattod.2013.10.058

Hayati-Ashtiani, M. (2011). Characterization of Nano-Porous Bentonite (Montmorillonite) Particles using FTIR and BET-BJH Analyses. Particle & Particle Systems Characterization, 28 (3-4), 71-76. https://doi.org/10.1002/ppsc.201100030

Khajeh Talkhoncheh, S., & Haghighi, M. (2015). Syngas production via dry reforming of methane over Ni-based nanocatalyst over various supports of clinoptilolite, ceria and alumina. Journal of Natural Gas Science and Engineering, 23, 16-25. https://doi.org/10.1016/j.jngse.2015.01.020

Li, L., Song, Y., Jiang, B., Wang, K., & Zhang, Q. (2017). A novel oxygen carrier for chemical looping reforming: $LaNiO_3$ perovskite supported on montmorillonite. Energy, 131, 58-66. https://doi.org/10.1016/j.energy.2017.05.030

Li, L., Tang, D., Song, Y., Jiang, B., & Zhang, Q. (2018). Hydrogen production from ethanol steam reforming on Ni-Ce/MMT catalysts. Energy, 149, 937-943. https://doi.org/10.1016/j.energy.2018.02.116

Li, T., Zhang, J., Xie, X., Yin, X., & An, X. (2015). Montmorillonite-supported Ni nanoparticles for efficient hydrogen production from ethanol steam reforming. Fuel, 143, 55-62. https://doi.org/10.1016/j.fuel.2014.11.033

Li, X., Tian, H., Zeng, L., Zhao, Z., & Gong, J. (2016). Dry reforming of methane over Ni/La_2O_3 nanorod catalysts with stabilized Ni nanoparticles. Applied Catalysis B: Environmental, 202, 683-694. https://doi.org/10.1016/j.apcatb.2016.09.071

Lu, M., Fang, J., Han, L., Faungnawakij, K., Li, H., & Cai, S. et al. (2018). Coke-resistant defect-confined Ni-based nanosheet-like catalysts derived from halloysites for CO_2 reforming of methane. Nanoscale, 10 (22), 10528-10537. https://doi.org/10.1039/C8NR02006J

Pugazhenthi, G., Suresh, K., Vinoth Kumar, R., Kumar, M., & Rajkumar Surin, R. (2018). A Simple Sonication Assisted Solvent Blending Route for Fabrication of Exfoliated Polystyrene (PS)/Clay Nanocomposites: Role of Various Clay Modifiers. Materials Today: Proceedings, 5 (5), 13191-13210. https://doi.org/10.1016/j.matpr.2018.02.310

Santhini, V., Sugunalakshmi, M., Suriyaraj, S., & Bava Bakrudeen, H. (2018). Carvedilol drug-organo montmorillonite nanocomposites: Preparation, characterization and drug release studies. Advanced Materials Letters, 9 (4), 258-265. https://doi.org/10.5185/amlett.2018.1881

Shin, S., Noh, Y., Hong, G., Park, J., Song, H., Lee, K., & Moon, D. (2018). Dry reforming of methane over Ni/ZrO_2 -Al_2O_3 catalysts: Effect of preparation methods. Journal of the

Taiwan Institute of Chemical Engineers, 90, 25-32. https://doi.org/10.1016/j.jtice.2017.11.032

Talaat Shawky, B. (2017). Conversion of rice straw to fermentable sugars and bioethanol by mfex pretreatment and sequential fermentation. Matter: International Journal of Science and Technology, 3 (2), 356-380. https://doi.org/10.20319/mijst.2017.32.356380

Wang, K., Dou, B., Jiang, B., Zhang, Q., Li, M., Chen, H., & Xu, Y. (2016). Effect of support on hydrogen production from chemical looping steam reforming of ethanol over Ni-based oxygen carriers. International Journal of Hydrogen Energy, 41 (39), 17334-17347. https://doi.org/10.1016/j.ijhydene.2016.07.261

YIN, X., XIE, X., WU, X., & AN, X. (2016). Catalytic performance of nickel immobilized on organically modified montmorillonite in the steam reforming of ethanol for hydrogen production. Journal of Fuel Chemistry and Technology, 44 (6), 689-697. https://doi.org/10.1016/S1872-5813(16)30033-0

Zhang, Q., Feng, X., Liu, J., Zhao, L., Song, X., Zhang, P., & Gao, L. (2018). Hollow hierarchical Ni/MgO-SiO_2 catalyst with high activity, thermal stability and coking resistance for catalytic dry reforming of methane. International Journal of Hydrogen Energy, 43 (24), 11056-11068. https://doi.org/10.1016/j.ijhydene.2018.05.010